Received: 23 August 2019 | Revised: 8 November 2019 | Accepted: 4 December 2019
DOI: 10.1002/aoc.5438

FULL PAPER

Applied Organometallic Chemistry WILEY

Transfer Hydrogenation of Nitroarenes Catalyzed by CoCu Anchored on Nitrogen-doped Porous Carbon

Xiaotong Liu[1] | **Longkang Zhang**[1] | **Junmin Wang**[1] | **Ningzhao Shang**[1] | **Shutao Gao**[1] | **Chun Wang**[1] | **Yongjun Gao**[2]

[1]College of Science, Hebei Agricultural University, Baoding, 071001, P. R. China

[2]College of Chemistry and Environmental Science, Hebei University, Baoding, 071002, China

Correspondence
Chun Wang, College of Science, Hebei Agricultural University, Baoding 071001, Hebei, China.
Email: chunwang69@126.com; wangchun@hebau.edu.cn

Yongjun Gao, College of Chemistry and Environmental Science, Hebei University, Baoding 071002, China.
Email: yjgao@hbu.edu.cn

Funding information
Natural Science Foundation of Hebei Province, Grant/Award Numbers: B2015204003, B2016204131, B2018204145, B2019204023; National Natural Science Foundation of China, Grant/Award Numbers: 21603054, 21773053

The non-precious metal catalysts with high catalytic activity is extremely desirable but still full of challenges. In this paper, CoCu bimetal immobilized on nitrogen-doped porous carbon (CoCu-N-C) was prepared by an effective ligand-stabilized pyrolysis strategy. CoCu-N-C exhibited excellent catalytic efficiency for the transfer hydrogenation of nitroarenes with ammonia borane as hydrogen source, which can be ascribed to the well dispersed metal nanoparticles, the synergetic interaction of CoCu bimetal and nitrogen-doped carbon. The durability and recyclability experiments of the recycled CoCu-N-C catalyst indicated that no obvious change in catalytic performance was observed after five consecutive cycles. To gain insight into the catalytic mechanism of CoCu-N-C for the hydrogenation reaction, density functional theory calculations was also conducted. This work provides an universal approach for constructing highly efficient non-precious metal heterogeneous catalysts and which may find diverse high performance applications.

KEYWORDS
ammonia borane, CoCu bimetaldensity functional theory, Nitroarene, transfer hydrogenation

1 | INTRODUCTION

Aromatic amine compounds are indispensable intermediates in the synthesis of various products including agrochemicals, pigments, dyes, polymers and pharmaceuticals.[1,2] A general synthetic route for aromatic amines is the catalytic hydrogenation of the corresponding nitroaromatic compound with hydrogen catalyzed by Pt, Pd, Au or other noble metal based nanoparticles.[3–5] Although hydrogenation with H_2 is considered as one of the most attractive approach, however, the reduction of nitroaromatic compounds with H_2 is usually performed at high pressure and high temperature. Meanwhile, H_2 is explosive, flammable and needs special equipments for production and transportation. Furthermore, not only the expensive price, but the limited reserve of noble metals impedes their industrial applications. On the other hand, the high catalytic activity of the noble metal-based catalysts usually resulted in high conversion but low selectivity.[6]

To avoid the employment of dangerous hydrogen, catalytic transfer hydrogenation (CTH), a much safer and environmental friendly method, has been proposed.[7] Among the hydrogen donors employed in CTH, ammonia-borane (AB) is a very potent hydrogen storage compound due to the high hydrogen capacity (19.6 wt%), excellent stability, low toxicity and high solubility in polar solvents, such as water and methanol.[8,9] Non-noble metal-based catalysts for CTH have received much interest due to its earth-abundant property and comparable catalytic performance with noble metal-based catalysts.[10–12] For example, Co–Mo_2C/AC developed by

https://doi.org/10.1002/aoc.5438

Guo et al exhibited unexpected catalytic performance for the facile and chemoselective reduction of nitroarenes.[13] Co/CN catalyst with Co^{2+} species on the catalyst surface can be applied as efficient heterogeneous catalyst for the transfer hydrogenation reactions with AB as hydrogen donor.[14] CuNi nanoparticles encapsulated in MIL-101 was fabricated by a double solvent approach followed by in situ reduction with NH_3BH_3, which exhibited good catalytic performance for the cascade reactions of nitroarene reduction.[15] Sun et al. assembled CuNi nanoparticles on graphene, which also displayed well catalytic activity for the nitroarene reduction[16]. Although significant progress has been achieved, these catalytic systems still have one or more limitations in terms of catalytic activity, stability, dispersity of the metal nanoparticles, recyclability and so on.[17–19] The development of highly selective, active, and stable heterogeneous catalysts for the catalytic transfer hydrogenation of nitroarenes under mild conditions is still desired urgently for practical use.

Transition metal supported on nitrogen-doped carbon (M-N-C) are demonstrated as promising catalysts for electrocatalysis and heterogeneous catalysis.[19–22] Nitrogen doping may serve as coordination sites for stabilizing the small size metal nanoparticles. Furthermore, the doped nitrogen may modulate the electronic structure of the nitrogen-doping carbon, which may regulate and improve the catalytic performance and selectivity of the M-N-C catalysts.[20,21] M-N-C catalysts are commonly prepared via pyrolyzing various nitrogen-containing precursors and metal salts at high temperature. However, the direct carbonization approaches usually cannot obtain highly dispersed metallic nanoparticles, which may deteriorate their catalytic activity. Although hard-template method may be a feasible process, however, it suffers from the disadvantages such as tedious synthesis processes and high cost. Moreover, it is usually required to remove the templates with hazard and toxic reagents. Another challenge is the large-scale production of the M-N-C catalysts, which is crucial to their practical applications. The method for mass preparation should be low cost, employing commercially available supports and scalable process. Therefore, a facile strategy compatible with mass production is still highly desirable to construct M-N-C catalysts.

In continuation of our efforts in exploring efficient heterogeneous catalysts,[22–25] we now report a versatile CoCu bimetal immobilized on nitrogen-doped porous carbon (CoCu-N-C) for the transfer hydrogenation reaction of nitroarenes. CoCu-N-C was prepared via an effective ligand-stabilized pyrolysis strategy. The CoCu-N-C catalyst displayed superior catalytic activity and stability for the CTH of nitro-compounds under mild conditions with AB as hydrogen donor. Density functional theory calculations revealed the important role of $M\text{-}N_x$ active sites for the excellent catalytic performance.

2 | EXPERIMENTAL SECTION

2.1 | Preparation of the catalysts

Cu $(NO_3)_2$•$3H_2O$(0.06 mmol), Co $(NO_3)_2$•$6H_2O$ (0.15 mmol) and 2,2′-dipyridyl (2 mmol) were dissolved in ethanol (50 ml) at room temperature with stirring for 10 min. Afterwards, Vulcan XC72R carbon (230 mg) was added into the above solution and the mixture was ultrasonicated for 30 min and stirred at 60 °C for 4 hr. The solvent was removed in vacuo. The dried sample was grinded to a fine powder. The sample was placed in a 60 degree oven for drying. The obtained black solid powder was sintered at 800 °C for 4 hr under Ar (5 °C/min ramp rate). The product was named as Co_5Cu_2-N1-C (the mol ratio of Co and Cu was 5:2). Co_2Cu_5-N1-C and Co_1Cu_1-N1-C were fabricated with the above procedure except that the mole ratio of Co and Cu was 2:5 and 1:1, respectively.

Co_5Cu_2-N2-C and Co_5Cu_2-C was prepared by the same method except that 1,10-phenanthroline was added instead of 2,2′-bipyridine and without addition of 2,2′-bipyridine, respectively. $^*Co_5{}^*Cu_2$-C was obtained with the same method except that 0.15 mmol cobalt acetylacetonate and 0.06 mmol copper acetylacetonate were added instead of Cu $(NO_3)_2$•$3H_2O$, Co $(NO_3)_2$•$6H_2O$ and 2,2′-bipyridine.

2.2 | Catalytic reduction of nitro-compounds

A mixture of nitro compound (0.2 mmol), ammonia-borane (0.8 mmol, 24.7 mg), catalyst (10 mg) and solvent (5 ml, EtOH:H_2O = 3:2, containing 0.2 mol/l NaOH) were added into a 25 ml round bottom flask. The flask was placed in a water bath at 30 °C with stirring and the reaction time was recorded. The reaction was monitored by TLC, upon completion of the reaction, the product was extracted with dichloromethane (3 x 5 ml) and quantified by gas chromatography (GC). The products were identified by comparison for their retention time with pure chemicals and further confirmed by GC–MS.

3 | RESULTS AND DISCUSSION

The catalyst preparation process was illustrated in Scheme 1. Vulcan XC-72R, a commercial available

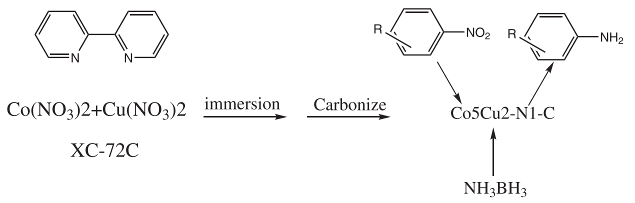

SCHEME 1 Schematic preparation process of CoCu-N-C

carbon material, possesses large specific surface area and high porosity, which make it an ideal candidate for catalyst support. Firstly, with the assistance of the ligands, the complex of Co $(NO_3)_2{\bullet}6H_2O$ and Cu $(NO_3)_2{\bullet}3H_2O$ with 2,2′-dipyridyl was anchored on the surface of Vulcan XC-72R carbon. After the solvent was removed in vacuo, the obtained composite was transferred to a ceramic boat in tube furnace and sintered at 800 °C for 4 hr under a pure Ar atmosphere. During the pyrolysis at high temperature, the chelating agent containing nitrogen can effectively sequester the metal ions and prevent the metal nanoparticles from aggregation. The well dispersed and nitrogen-doped carbon shell encapsulated CoCu bimetallic catalyst (CoCu-N1-C) was finally obtained.

For comparison, Co_5Cu_2-N2-C, $^*Co_5{}^*Cu_2$-C and Co_5Cu_2-C were also prepared with 1,10-phenanthroline, acetylaceton as the ligand, and without the addition of a ligand, respectively (see details in Experiment section).

3.1 | Characterization of the materials

The structure and morphology of the as-obtained catalysts were characterized by TEM. Figure 1a showed that fine crystalline of CoCu nanoparticles in Co_5Cu_2-N1-C sample were evenly dispersed on the support with an average diameter of about 11 nm. As shown in Figure 1b and 1c, the TEM images obvious revealed that CoCu nanoparticles were encapsulated in the lattice fringes of graphite carbon. The high-resolution TEM image (Figure 1c) displayed that the lattice fringes of the encapsulated nanoparticles were 0.208 nm, which was attributable to the (111) plane of fcc Co or Cu due to the similarity of the lattice constants of Co and Cu[26]. It can be seen from Figure 1c that the thickness of the carbon shell was between 4 and 7 nm, and the lattice fringes of 0.338 nm matched the (002) plane of graphite carbon.[27] Elemental mapping images of Co_5Cu_2-N1-C obviously confirmed that Co, Cu and N were uniformly distributed on the catalyst. There was some copper signal noise outside the metal particles. This was due to the copper mesh

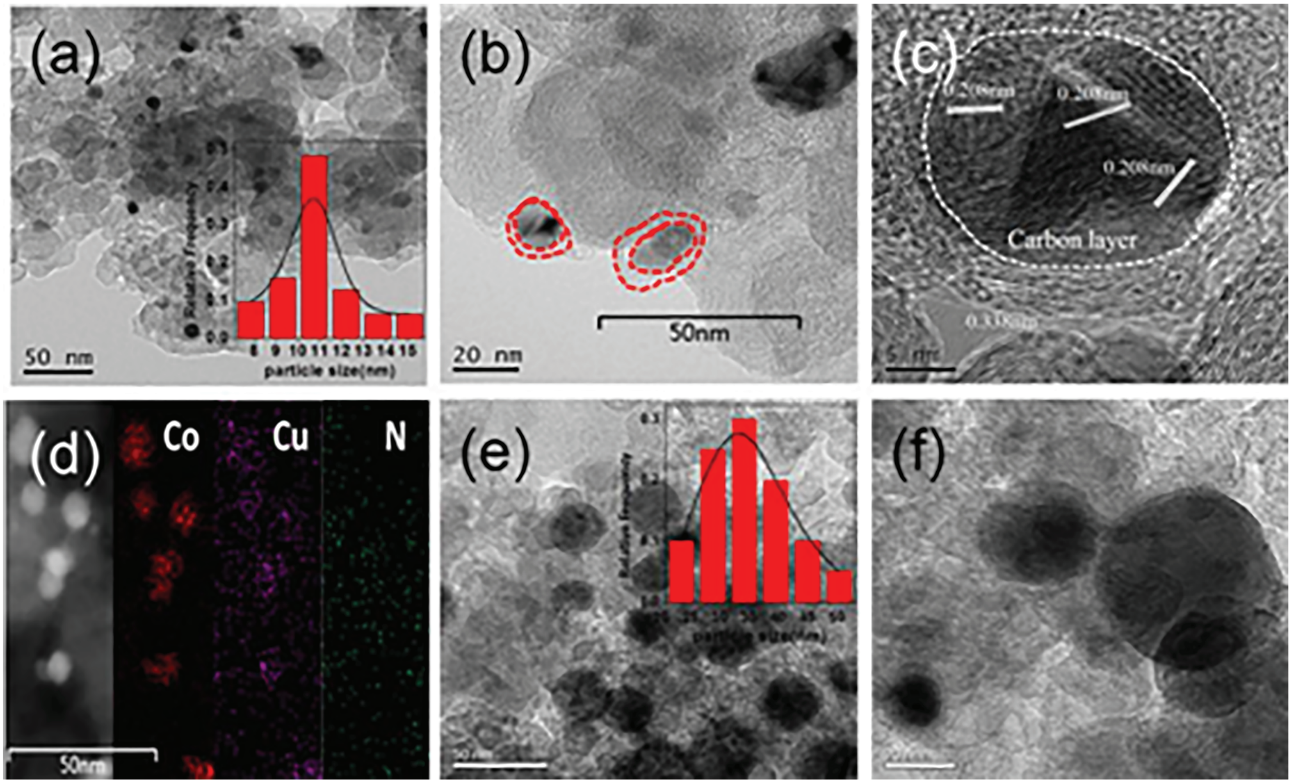

FIGURE 1 TEM images of Co_5Cu_2-N1-C catalyst (a, b and c) and corresponding size distribution of Co_5Cu_2 nanoparticles, element mappings of Co, Cu and N in Co_5Cu_2-N1-C (d), TEM images of Co_5Cu_2-C catalyst (e and f) and corresponding size distribution of Co_5Cu_2 nanoparticles

used as sample support for TEM analysis. (Figure 1d)[28]. In contrast, for Co_5Cu_2-C sample prepared without addition of a nitrogen-containing ligand, the size of the bimetallic nanoparticles is relatively large, and the diameter of the metal particles was approximately 30 nm to 40 nm (as shown in Figure 1e). No clear carbon layers over the Cu-Co bimetallic nanoparticles can be observed (Figure 1f). These results indicated that a graphite carbon shell was formed in Co_5Cu_2-N1-C by direct pyrolysis of the nitrogen-rich metal complex, which not only prevented the aggregation of metal nanoparticles, but also the nitrogen-containing species can stabilize the small size metal nanoparticles. The content of cobalt and copper in Co_5Cu_2-N1-C was 4.37 wt% and 1.78 wt%, respectively, which were determined by inductively coupled plasma atomic emission spectrometry (ICP-AES).

To confirm the electronic structures of Cu-Co based metal/metal oxide nanoparticles in Co_5Cu_2-N1-C, XPS was carried out. Based on the XPS data, atomic information of C, Co, Cu, and N can be obtained. The three peaks centered at 289.0 285.5 and 284.6 eV were attributed to C − N bonds, sp^3-hybridized diamond-like carbon and sp^2-hybridized graphite-like carbon, respectively (Figure 2a).[29] The signal of Co and Cu were weak, probably because CoCu were covered by carbon shell. The Co 2p emission spectrum of Co_5Cu_2-N1-C (Figure 2b) indicated two main signals located at 780 and 796 eV, corresponding to Co $2p_{3/2}$ and Co $2p_{1/2}$, respectively, and weak satellite peaks located at around 786 and 805 eV. The binding energies at 780.4, 781.9 and 786.8 eV can be attributed to Co $2p_{3/2}$ peak. The binding energy of 780.4 eV was assigned to the cobalt coordinate with pyridinic N to form catalytically active Co-Nx sites. The energy at 781.9 eV was attributed to the metallic Co(0) element.[30] The XPS peaks of Cu $2p_{3/2}$ and $2p_{1/2}$ at the binding energy of 933 eV and 953 eV can be classified into four types. The peaks observed at 932.9 eV and 952.6 eV were assigned to metallic Cu(0). The peaks at 934.6 eV and 954.5 eV were corresponding to Cu^{2+}-N_x[31,32].

However, compared with Co_5Cu_2-C and Co_5Cu_2-N2-C (with 1,10-phenanthroline as the ligand) catalysts, the Co peak of Co_5Cu_2-N1-C shifted to a lower binding energy due to the close coupling of Co and N atoms, which indicated the electrons of N transferred to the cobalt (Figure S1). Therefore, the electron distribution on the catalyst surface was modulated, which was beneficial to the catalytic reaction.[33] The N 1 s XPS spectrum of the catalyst can be deconvoluted into three peaks at

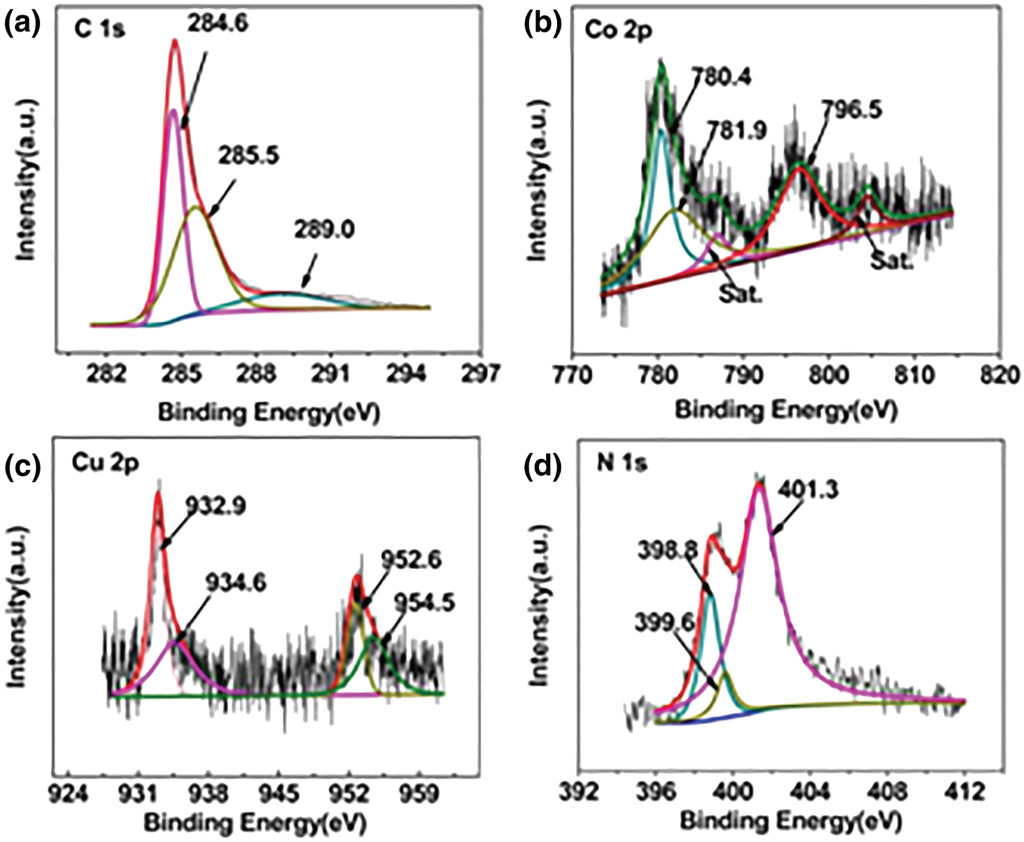

FIGURE 2 XPS data of Co_5Cu_2-N1-C catalyst. High-resolution spectrum of C 1 s (a), Co 2p (b), Cu 2p (c) and N 1 s (d)

398.8, 399.6 and 401.3 eV, which were corresponded to pyridine N, pyrrole N and graphite N, respectively. The nitrogen species may coordinated with copper and cobalt. Moreover, according to the previous reported results, pyrrolic N species had strong ability to absorb and activate nitro compounds, and induce favorable energetic charges in heterogeneous catalytic processes.[31,34]

The XRD patterns of the samples were investigated, a pronounced diffraction peak at 26° appeared in all samples due to the (002) reflection of the graphite type lattice (Figure 3a). Sample presents three peaks at $2\theta = 44.1°$, 51.5° and 75.8°, which was assigned to the cobalt (111), (200) and (220) diffraction peak (PDF#15–0806). The main characteristic of copper (111), (200), and (220) were observed at 43.2°, 50.4°, and 74.1° (PDF#04–0836). For the Co_5Cu_2-N1-C sample, we can see the obvious peaks of Co and Cu at 44.1°, 51.5°, 43.2°, 50.4°, indicating the formation of CoCu composite, which was consistent with the results of the electron micrograph. Compared with the XRD patterns of Co_5Cu_2 alloy, the results also demonstrated that CoCu in the Co_5Cu_2-N1-C sample was not an alloy structure. Typical N_2 adsorption–desorption isotherms of the samples were shown in Figure 3b. All samples displayed H_3-type hysteresis loop and a type-IV curve, indicating the mesoporous structure of the prepared samples, which is confirmed by the pore size distribution curve (Figure 3c). The surface area of Co_5Cu_2-C, Co_5Cu_2-N1-C, XC-72R and N1-C were 207, 77, 253 and 106 $m^2\ g^{-1}$, respectively.

3.2 | The catalytic hydrogenation of nitroarenes

In order to study the catalytic performance of the prepared catalysts, the CTH of 4-nitrochlorobenzene with AB as the hydrogen donor were used as the model reaction. We screened the reaction conditions for the formation of p-chloroaniline and listed them in Table 1. XC-72R and N1-C did not give a conversion of 4-nitrochlorobenzene, indicating that the support material was not active against the reduction of 4-nitrochlorobenzene under the conditions studied. (Table 1, entries 1 and 2). Co_5Cu_2-C and $*Co_5*Cu_2$-C prepared without nitrogen-containing precursors exhibited much low activity on the reaction (Table 1, entries 3 and 4). Adding nitrogen-containing ligands can significantly improved the catalytic activity of the catalyst, Co_5Cu_2-N1-C prepared with 2,2′-dipyridyl as the ligand delivered excellent catalytic performance for the CTH of 4-nitrochlorobenzene. The experimental results showed that near complete conversion and 99% selectivity were obtained after 15 min at 30 °C (Table 1, entry 5). Compared with the reported catalysts in the literatures, Co_5Cu_2-N1-C delivered the highest activity except the precious metal catalyst (Table S1). However, the Co_5Cu_2-N2-C catalyst prepared with phenanthroline as the ligand can only achieve 69% selectivity after 30 min reaction although 99% conversion can be achieved (Table 1, entry 6). These results indicated that the structure of the nitrogen precursor plays an important role in the catalytic performance of the catalysts. For comparison, Cu-N1-C, Co-N1-C, Co_2Cu_5-N1-C and Co_1Cu_1-N1-C catalysts were also fabricated. However, the selectivity of Cu-N1-C and Co-N1-C was relatively low (Table 1, entries 7–8). Compared with Co_5Cu_2-N1-C, the catalytic selectivity of Co_2Cu_5-N1-C and Co_1Cu_1-N1-C decreased slightly with increasing the amount of Cu in the catalysts (Table 1, entries 9–10). The above results clearly demonstrated that the synergetic interaction of Cu and Co also responsible for the excellent activity of Co_5Cu_2-N1-C.

We also studied the effects of the type of solvents on the reaction. The results showed that the solvent has an important influence on the catalytic reaction (Table 1, entries 11–14). Due to the poor solubility of nitroarene in water, the conversion of 4-nitrochlorobenzene was only 25% after 30 min reaction under the same reaction conditions with water as solvent (entry 14). When MeOH,

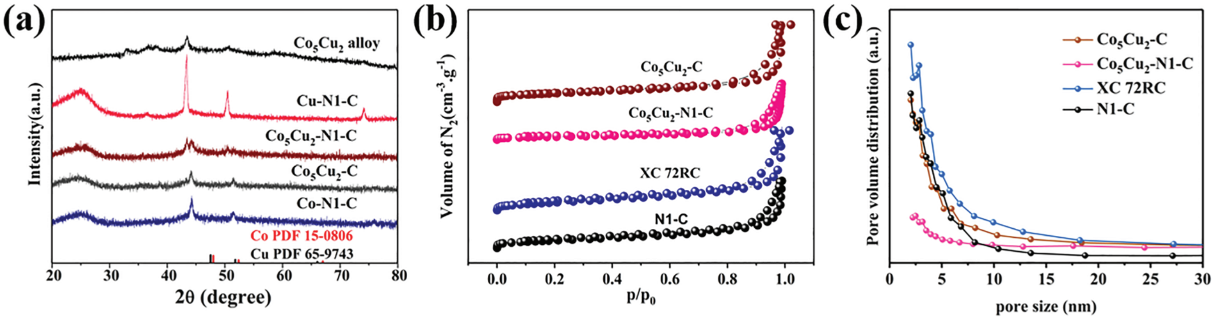

FIGURE 3 (a) XRD images of different catalysts, (b) The N_2 adsorption–desorption isotherms of Co_5Cu_2-N1-C, Co_5Cu_2-C, N1-C and XC-72R carbon

TABLE 1 Screening of catalysts

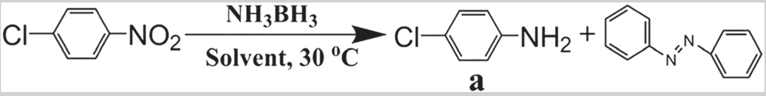

Entry	Catalysts	Solvents	Time (min)	Con (%)	Sel(a) (%)
1	XR-72R	EtOH:Water (3:2)	60	-	-
2	N1-C	EtOH:Water (3:2)	60	-	-
3	*Co_5*Cu_2-C	EtOH:Water (3:2)	30	3	87
4	Co_5Cu_2-C	EtOH:Water (3:2)	30	4	79
5	Co_5Cu_2-N1-C	EtOH:Water (3:2)	15	99	99
6	Co_5Cu_2-N2-C	EtOH:Water (3:2)	30	99	69
7	Cu-N1-C	EtOH:Water (3:2)	30	99	77
8	Co-N1-C	EtOH:Water (3:2)	30	75	70
9	Co_1Cu_1-N1-C	EtOH:Water (3:2)	30	99	95
10	Co_2Cu_5-N1-C	EtOH:Water (3:2)	30	99	82
11	Co_5Cu_2-N1-C	EtOH	30	99	94
12	Co_5Cu_2-N_1-C	MeOH	30	99	56
13	Co_5Cu_2-N1-C	MeOH:Water (3:2)	30	99	88
14	Co_5Cu_2-N_1-C	Water	30	25	99
15[b]	Co_5Cu_2-N1-C	EtOH:Water (3:2)	5	99	99
16[c]	Co_5Cu_2-N1-C	EtOH:Water (3:2)	30	83	99
17[d]	Co_5Cu_2-N1-C	EtOH:Water (3:2)	5	99	99
18[e]	Co_5Cu_2-N1-C	EtOH:Water (3:2)	30	92	73

*Reaction conditions: ammonia borane (0.8 mmol), 4-nitrochlorobenzene (0.2 mmol), catalyst (5 mol%), solvent (5 ml, containing 0.2 mol/l NaOH), 30 °C. [b]ammonia borane(1.6 mmol), [c]ammonia borane (0.4 mmol), [d]catalyst (10 mol%), [e]catalyst (2.5 mol%).

MeOH:Water (3:2), EtOH and EtOH:Water (3:2) were employed as the solvent, 99% conversion was achieved due to the good solubility of nitroarene in these solvents, the selectivity was 56%, 88%, 94% and 99% (entries 5, 11–13), respectively. The difference of selectivity may related to the polarity of the solvents and the solubility of the products and the reaction intermediates. When the dosage of the catalyst and ammonia borane increased, the reaction can be completed in 5 min (Table 1, entries 15 and 17). When we reduced the amount of catalyst and ammonia borane, only a conversion of 83% and 92% was obtained after 30 min, respectively (Table 1, entries 16 and 18). Changing the concentration of sodium hydroxide has a great influence on the reaction rate and selectivity. Perhaps the presence of hydroxide accelerates the hydrogen production of AB and competes with transfer hydrogenation (Figure S2). However, the reason for the improved activity in the presence of extra OH^- was still unclear.[35]

The reusability of Co_5Cu_2-N1-C was tested by using CTH and AB of 4-nitrochlorobenzene as a model reaction. The resulted showed that the recycled Co_5Cu_2-N1-C catalyst can maintain a conversion of 4-nitrochlorobenzene greater than 95% in 15 min under the same reaction conditions even after seven runs (Figure S3). The TEM image of the recycled catalyst showed no significant agglomerate after seven runs compare with the fresh catalyst and still maintained its excellent dispersity (Figure S4). The XRD pattern showed no obvious difference between the fresh catalyst and the reused catalyst up to 7 runs (Figure S5). The results clearly demonstrated that the prepared catalyst has high durability and stability.

To further elucidate the heterogeneous nature of the catalyst, a hot leaching experiment was performed. After the hydrogenation of 4-nitrochlorobenzene was conducted for 5 min, the Co_5Cu_2-N1-C catalyst was filtered out from the reaction solution and the filtrate was allowed to react for 30 min, negligible changes in conversion was observed (Figure S6). The experimental results show that metal leaching did not occur and the reaction was predominantly heterogeneous.

In order to further prove the universal applicability of the catalyst, various nitroaromatic hydrocarbons were

TABLE 2 Reduction of nitro compounds to corresponding amines

Entry	Substrates	Products	Time (min)	Con. (%)	Sel. (%)
1	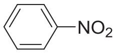	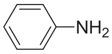	2	99	99
2	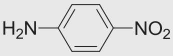		1	99	99
3	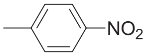	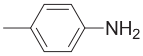	2	99	99
4	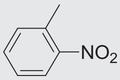	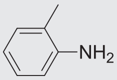	2	99	99
5	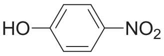	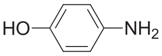	2	99	99
6	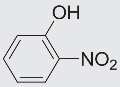	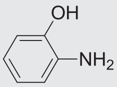	2	99	99
7	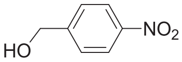	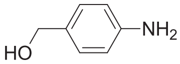	1	99	99
8	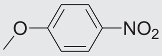	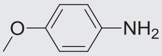	2	99	99
9	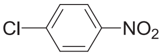	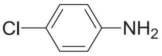	15	99	99
10	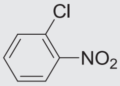	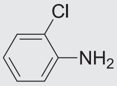	30	99	99
11	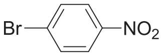	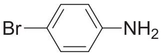	30	99	99
12	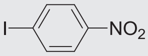	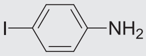	30	99	79
13	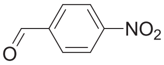	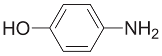	2	99	99
14	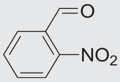	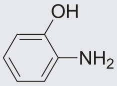	4	99	99
15	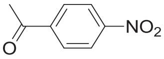	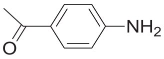	2	99	99

(Continues)

TABLE 2 (Continued)

Entry	Substrates	Products	Time (min)	Con. (%)	Sel. (%)
16	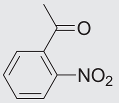	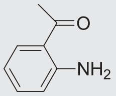	5	99	99
17	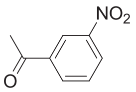	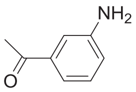	4	99	99
18	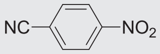	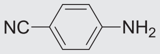	30	99	75
19	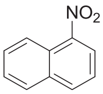	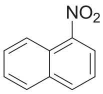	30	99	88

*Reaction conditions: ammonia borane (0.8 mmol), nitroaromatics (0.2 mmol), catalyst (5 mol %), ethanol-water (3:2), (5 ml, containing 0.2 mol/l NaOH), 30 °C.

subjected to CTH over Co_5Cu_2-N1-C catalyst under the optimized reaction conditions. It is gratifying to find that the catalyst has high activity not only for nitrobenzene (Table 2, entry 1), but also for other nitro compounds with electron donor substituents, such as $-NH_2$, $-CH_3$, -OH, CH_3O-, $HOCH_2$- (Table 2, entries 2–8). These substrates gave 99% yields and high selectivity in less than 2 min. The choice of substituents with steric hindrance (Table 2, entries 3 and 6) didn't interfere with the activity of the catalyst. It was noteworthy that the halogen-substituted nitrobenzene was reduced to the corresponding aniline in excellent yield without any dehalogenation (Table 2, entries 9–12). It is worth noting that even unstable labilebromide- and iodo-nitroarenes were selectively hydrogenated with a selectivity of 99% and 79% in 30 min, respectively (Table 2, entries 11 and 12). In particular, carbonyl functionalized nitroaromatics (e.g., aldehydes and ketones) were successfully reduced to the aniline product with a yield of up to 99% in 5 min (Table 2, entries 13–17), but lost selectivity for nitrobenzaldehydes in which aldehyde groups were also reduced (Table 2, entries 13–14). The position of the aldehyde and ketone substituent does not significantly affect the reactivity (Table 2, entries 14, 16 and 17). *p*-Nitrobenzonitrile was reduced to the corresponding amine products with 75% selectivity (Table 2, entry 18). Finally, we tested the hydrogenation of 1-nitronaphthalene and 88% selectivity was obtained (Table 2, entry 18).

3.3 | DFT calculations

The high catalytic activity of CoCu-N-C can be also revealed from density functional theory (DFT) calculations. The adsorption of nitrobenzene on CoCu-N-C catalyst

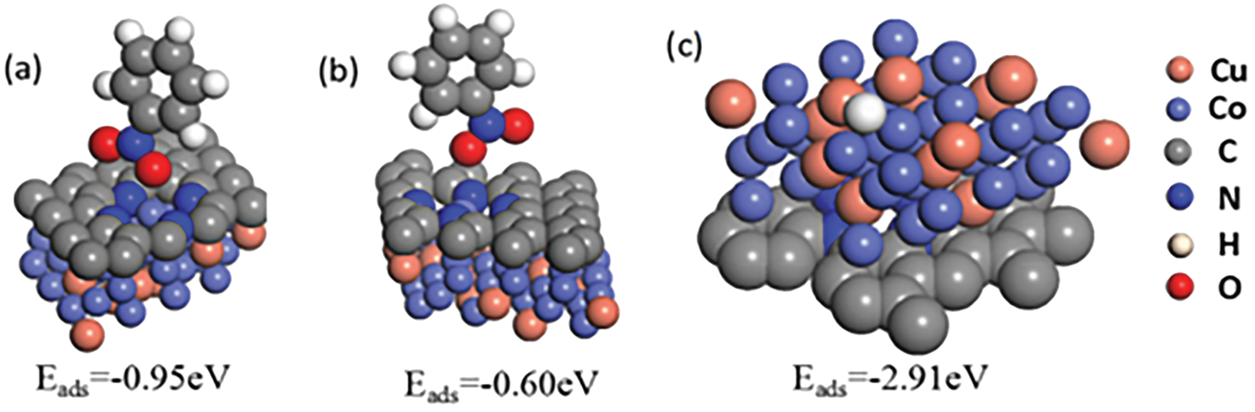

FIGURE 4 Summary of adsorption models of nitrobenzene on CoCu-N-C surface (a, b) and H atoms are located in the triangular voids formed by CuCo nanocluster (c)

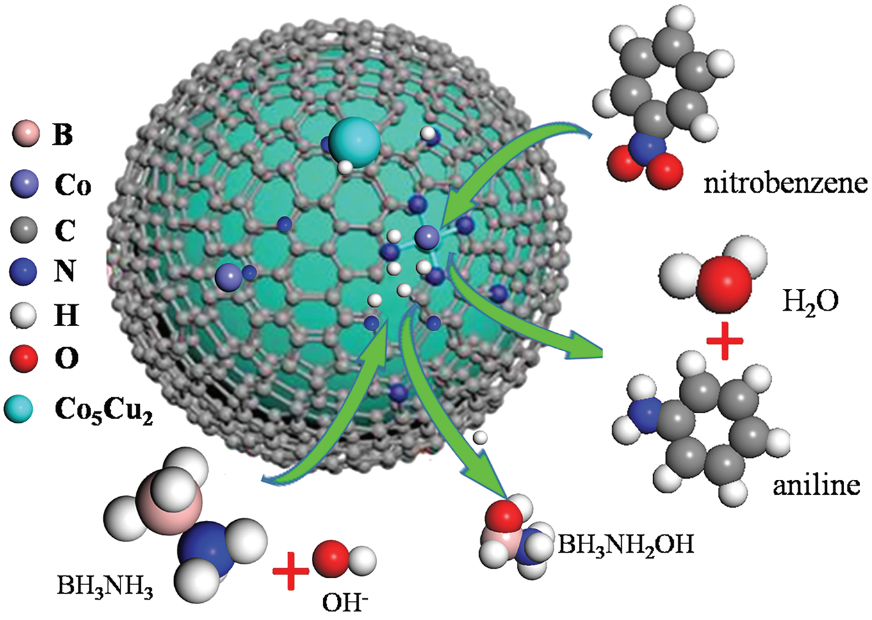

FIGURE 5 Proposed catalytic process for hydrogenation of nitrobenzene catalyzed by the CoCu-N-C catalyst

was verified and there are two adsorption site, CoN_x sites and nitrogen sites, on the surface of the catalyst. The CoCu-N-C catalyst acts as an electron donor, and the oxygen atom (O) in nitrobenzene acts as an electron acceptor. Figure 4 showed the optimized configurations for the adsorption of nitrobenzene on the CoCu-N-C catalyst. The adsorption ability of nitrobenzene on CoN_x site of CoCu-N-C was the strongest, the adsorption energy was −0.95 eV. The length of N − O bond in nitrobenzene can be extended to 1.281 Å compared with the intrinsic length of N − O (1.237 Å) .

To illustrate the origin of the improved catalytic activity, the electronic structures of the catalyst were investigated. Bader charges of Co atom in CoN_x were listed in Table S2. The results indicated that there is net 0.04e electron transfer when Co nanoparticles were absorbed on CoN_xC (CoN_xC@Co), and 0.05e electron transfer when Co_5Cu_2 nanoparticles absorbed on CoN_xC (CoN_xC@CoCu), so there was additional 0.01e electron transfer because of the introduction of copper atom. There was 0.19e electron transfer from Co atom to O atom when nitrobenzene was absorbed on the catalyst.

According to the reaction mechanism of AB dehydrogenation, AB was adsorbed on the catalyst firstly to produce H radical. To further investigate the activity origin, the adsorption ability of the active sites for H radical were calculated by DFT. Figure 4c and Figure S7 showed the different atomic configurations of H radical on Co(111)-N-C, Cu(111)-N-C, CoCu-N-C, respectively. Among them, the bridge adsorption of H on CoCu-N-C catalyst possessed the strongest adsorption ability, the shortest distance (1.65 Å) between H to metal nanoparticles and the highest adsorption energy (−2.91 eV). H atoms were located in the triangular voids of CuCo nanocluster.

Based on the above investigations, we proposed a tentative multiple-catalytic-sites mechanism for the reduction reaction of nitrobenzene catalyzed by the CoCu-N-C catalyst, which was displayed in Figure 5. Firstly, nitrobenzene preferred to bond on the CoN_x site and dipyridyl N accompanying with fast electron accumulation. Meanwhile, H was adsorbed on the multiple sites of CoCu-N-C. The multiple reaction sites greatly reduced the migration distance for the active reaction species and thus improved the catalytic performance of CoCu-N-C.

4 | CONCLUSIONS

In summary, CoCu bimetal immobilized on nitrogen-doped porous carbon prepared by an effective ligand-stabilized pyrolysis strategy. The optimized Co_5Cu_2-N1-C nanocatalyst exhibited excellent activity for the CTH of nitro compounds. Both the experimental and DFT calculation results revealed the important role of M-N active sites for the excellent catalytic performance. This research presented a feasible and universal strategy to design high-performance non-precious metal catalysts for the hydrogenation of nitro compounds, and will inspire the development of non-precious metal-based heterogeneous catalysts.

ACKNOWLEDGMENTS

This work was financially supported by the National Natural Science Foundation of China (21773053, 21603054), the Natural Science Foundation of Hebei

Province (B2019204023, B2018204145, B2016204131, B2015204003).

ORCID

Longkang Zhang https://orcid.org/0000-0002-1934-9718
Ningzhao Shang https://orcid.org/0000-0001-9070-0024
Chun Wang https://orcid.org/0000-0002-9366-3668

REFERENCES

[1] P. Zhou, Z. Zhang, *ChemSusChem* **2017**, *10*, 1892.

[2] X. Li, Z. Wang, S. Mao, Y. Chen, M. Tang, H. Li, Y. Wang, *Chin. J. Chem.* **2019**, *3*, 1191.

[3] T. Mitsudome, K. Kaneda, *Green Chem.* **2013**, *15*, 2636.

[4] Q. Yang, Y. Z. Chen, Z. U. Wang, Q. Xu, H. L. Jiang, *Chem. Commun.* **2015**, *51*, 10419.

[5] L. Yu, Q. Zhang, S. Li, J. Huang, Y. Liu, H. He, Y. Cao, *ChemSusChem* **2015**, *8*, 3029.

[6] Z. Liu, X. Wang, X. Zou, X. Lu, *ChemistrySelect* **2018**, *3*, 5165.

[7] Q. Yao, Z. Lu, W. Huang, X. Chen, J. Zhu, J. Mater, *Chem. A* **2016**, *4*, 8579.

[8] J. S. Samec, J.-E. Bäckvall, P. G. Andersson, P. Brandt, *Chem. Soc. Rev.* **2006**, *35*, 237.

[9] D. Wang, D. Astruc, *Chem. Rev.* **2015**, *115*, 6621.

[10] R. V. Jagadeesh, G. Wienhoefer, F. A. Westerhaus, A. E. Surkus, M. M. Pohl, H. Junge, K. Junge, M. Beller, *Chem. Commun.* **2011**, *47*, 10972.

[11] F. Zhang, C. Zhao, S. Chen, H. Li, H. Yang, X. Zhang, *J. Catal.* **2017**, *348*, 212.

[12] A. Staubitz, A. P. Robertson, I. Manners, *Chem. Rev.* **2010**, *110*, 4079.

[13] Z. Zhao, H. Yang, Y. Li, X. Guo, *Green Chem.* **2014**, *16*, 1274.

[14] T.-J. Zhao, Y.-N. Zhang, K.-X. Wang, J. Su, X. Wei, X.-H. Li, *RSC Adv.* **2015**, *5*, 102736.

[15] Y. Zhou, Q. Yang, Y.-Z. Chen, H. Jiang, *Chem. Commun.* **2017**, *53*, 12361.

[16] C. Yu, J. Fu, M. Muzzio, T. Shen, D. Su, J. Zhu, S. Sun, *Chem. Mater.* **2017**, *29*, 1413.

[17] Z. Wu, S. Xu, Q. Yan, Z. Chen, Y. Ding, C. Li, H. Liang, S. Yu, *Sci. Adv.* **2018**, *4*, eaat0788.

[18] F. A. Westerhaus, R. V. Jagadeesh, G. Wienhofer, M. M. Pohl, J. Radnik, A. E. Surkus, J. Rabeah, K. Junge, H. Junge, M. Nielsen, A. Bruckner, M. Beller, *Nat. Chem.* **2013**, *5*, 537.

[19] R. V. Jagadeesh, T. Stemmler, A. E. Surkus, M. Bauer, M. M. Pohl, J. Radnik, K. Junge, H. Junge, A. Brückner, M. Beller, *Nat. Protoc.* **2016**, *11*, 192.

[20] S. Mao, C. Wang, Y. Wang, *J. Catal.* **2019**, *375*, 456.

[21] Y. Chen, Z. Wang, S. Mao, Y. Wang, *Chin. J. Catal.* **2019**, *40*, 971.

[22] J. Li, L. Zhang, X. Liu, N. Shang, S. Gao, C. Feng, C. Wang, Z. Wang, *New J. Chem.* **2018**, *42*, 9684.

[23] J. Li, S. Cheng, T. Du, N. Shang, S. Gao, C. Feng, C. Wang, Z. Wang, *New J. Chem.* **2018**, *42*, 9324.

[24] X. Liu, C. Wang, S. Cheng, N. Shang, S. Gao, C. Feng, C. Wang, Y. Qiao, Z. Wang, *Cat. Com.* **2018**, *108*, 103.

[25] S. Cheng, N. Shang, X. Zhou, C. Feng, S. Gao, C. Wang, Z. Wang, *New J. Chem.* **2017**, *41*, 9857.

[26] Y. Xiang, R. Barbosa, N. Kruse, *ACS Catal.* **2014**, *4*, 2792.

[27] Y. Zhang, L. Lu, S. Zhang, Z. Lv, D. Yang, J. Liu, Y. Chen, X. Tian, H. Jin, W. Song, J. Mater, *Chem. A* **2018**, *6*, 5740.

[28] B. Chen, F. Li, Z. Huang, G. Yuan, *Appl. Catal. B-Environ.* **2017**, *200*, 192.

[29] P. Zhou, Z. Zhang, L. Jiang, C. Yu, K. Lv, J. Sun, S. Wang, *Appl. Catal. B-Environ.* **2017**, *210*, 522.

[30] H. Jiang, Y. Liu, W. Li, J. Li, *Small* **2018**, *14*, 1703739.

[31] T. Song, P. Ren, Y. Duan, Z. Wang, X. Chen, Y. Yang, *Green Chem.* **2018**, *20*, 4629.

[32] X. Wei, Z. Zhang, M. Zhou, A. Zhang, W. D. Wu, Z. Wu, *Nanoscale* **2018**, *10*, 16839.

[33] X. Wang, Y. Li, *J. Mol. Catal. a: Chem.* **2016**, *420*, 56.

[34] G. Huang, L. Yang, X. Ma, J. Jiang, S. Yu, H. Jiang, *Chemistry* **2016**, *22*, 3470.

[35] C. Hou, Q. Li, C. Wang, C. Peng, Q. Chen, H. Ye, W. Fu, C. Che, N. López, Y. Chen, *Energy Environ. Sci.* **2017**, *10*, 1770.

SUPPORTING INFORMATION

Additional supporting information may be found online in the Supporting Information section at the end of this article.

How to cite this article: Liu X, Zhang L, Wang J, et al. Transfer Hydrogenation of Nitroarenes Catalyzed by CoCu Anchored on Nitrogen-doped Porous Carbon. *Appl Organometal Chem*. 2020; e5438. https://doi.org/10.1002/aoc.5438